Journal of Physics B: Atomic, Molecular and Optical Physics

PAPER • OPEN ACCESS

Magnetic field-free measurements of the total cross section for positrons scattering from helium and krypton

To cite this article: S E Fayer *et al* 2016 *J. Phys. B: At. Mol. Opt. Phys.* **49** 075202

OPEN ACCESS
IOP Publishing
Journal of Physics B: Atomic, Molecular and Optical Physics
J. Phys. B: At. Mol. Opt. Phys. **49** (2016) 075202 (6pp)
doi:10.1088/0953-4075/49/7/075202

Magnetic field-free measurements of the total cross section for positrons scattering from helium and krypton

S E Fayer[1], A Loreti[1], S L Andersen[2], Á Kövér[3] and G Laricchia[1]

[1] UCL Department of Physics and Astronomy, University College London, Gower Street, London WC1E 6BT, UK
[2] Department of Physics and Astronomy, Aarhus University, DK-8000 Aarhus C, Denmark
[3] Institute for Nuclear Research of Hungarian Academy of Science, Debrecen, PO Box 51, H-4001, Hungary

E-mail: g.laricchia@ucl.ac.uk

Received 14 January 2016, revised 12 February 2016
Accepted for publication 24 February 2016
Published 17 March 2016

Abstract
An electrostatic beam has been used to perform scattering measurements with an angular-discrimination of $\lesssim 2°$. The total cross sections of positrons scattering from helium and krypton have been determined in the energy range (10–300) eV. This work was initially stimulated by the investigations of Nagumo *et al* (2011 *J. Phys. Soc. Japan* **80** 064301), the first positron field-free measurements performed with a similarly high resolution, which found significant discrepancies at low energies with most other experiments and theories. The present results show good agreement with theories and several other measurements, even those characterized by a much poorer angular discrimination, implying a small contribution from particles elastically scattered at forward angles, as theoretically predicted for He but not for Kr.

Keywords: positron beam, brightness enhancement, electrostatic transport, positron scattering, helium, krypton, total cross section

(Some figures may appear in colour only in the online journal)

Introduction

Considerable progress in the understanding of the interactions of antimatter with matter has been achieved through the study of low energy collisions of positrons (e^+) and positronium (Ps) with atoms and molecules (e.g. [1–5]), assisting advances of accurate scattering theories (e.g. [1, 2, 5–7]), precision tests of QED bound-state problems (e.g. [8–10]), analyses of astrophysical and atmospheric events (e.g. [11, 12]), and positron-track simulations of relevance in biomedical applications (e.g. [13, 14]).

The opposite signs of the static and polarization interactions for positrons tend to reduce their scattering probability at low energies in comparison to electrons (e.g. [15]), despite the presence of extra channels (annihilation and Ps formation) available to positrons in encounters with matter. Annihilation is considered generally negligible, except in the limit of zero velocity relative to that of an electron (e.g. [16]) or by attachment (e.g. via vibrational Feshbach resonances [2, 17]). Ps formation, however, may account for up to ~50% of the total scattering probability and be a significant channel even when formation occurs in an excited-state [18] or accompanied by excitation of the residual ion [19]. Polarization often enhances positron-impact direct ionization (e.g. [20]), so that the total ionization cross-section by e^+ may exceed that by electrons [3].

The present work was initially stimulated by the total cross section results for positrons colliding with helium [21] and neon [22] determined for the first time in the absence of a magnetic field, employed for beam transport in all previous

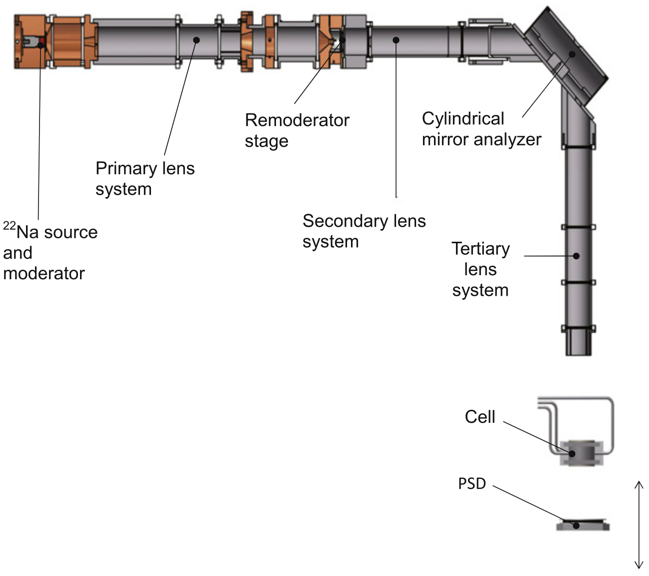

Figure 1. Schematic of the electrostatic beam used in this experiment.

experiments. Significant discrepancies were found between (3–20) eV with earlier results and, given that in transmission experiments, a major source of systematic error arises from ascribing particles elastically scattered to small forward angles (FSP) to the unscattered beam, it was noted that the high (energy-independent) angular resolution associated with electrostatic systems should help to minimize this effect.

In the current experiment, the total cross sections for positron scattering from helium and krypton have also been performed in a field-free region using an electrostatic beam transport. Measurements have been obtained in a range of energies between (10–300) eV and are here compared with previous experimental and theoretical results.

Experimental apparatus

The equipment used for this experiment is illustrated in figure 1 and has been described in detail elsewhere [23]. Briefly, positrons from a ^{22}Na source are moderated by a stack of three annealed tungsten meshes (20 μm wire and 70% transmission) [24]. A set of primary lenses transports the beam at 2 keV from the moderator and focus it to a small beam spot of radius ~1 mm at the re-moderator. This is an annealed W(100) foil (thickness ≃50 nm) with a remoderation efficiency of 0.1 [23]. The re-moderator is floated at a potential (V_{Rm}) to accelerate the positrons to the required beam energy ($E_+ = eV_{\mathrm{Rm}} + |\phi|$), where $\phi = -2.7 \pm 0.1$ eV is the positron work function for the current re-moderator [23] and e is the positron electric charge. The positrons are then transported around a 90° corner through a cylindrical mirror analyser before reaching the interaction region.

An aluminium cylindrical cell is situated after the exit lenses. It has a length of $L = 53$ mm and inner radius 25.4 mm. Two aperture radii were used ($R_{\mathrm{a}} = 0.5$ mm and 1 mm for He and Kr, respectively) in order to retain a high angular discrimination and a sharp gas density profile [25]. A position sensitive detector (PSD) terminates the flight path, approximately 130 mm from the entrance aperture of the cell. Beam rates through the 1 mm radius cell apertures were in the range $(3 - 3.6)e^+s^{-1}$ at 100 eV and $(0.01 - 0.05)e^+s^{-1}$ at 10 eV during the course of the experiment, and approximately a quarter of these for the smaller apertures.

In front of the detector, two grids are mounted that enable retarding potential analysis (RPA) and are also used, during the total cross section measurements, to reflect inelastically forward scattered particles. The beam has an angular divergence of 1° and longitudinal energy spread of 1% [23]. The angular acceptance is set by geometrical constraint[3], $\theta = \arctan[R_{\mathrm{a}}/(L/2)] \lesssim 2°$. A comparison between some of the characteristics of the current and previous experimental set-ups is made in table 1.

The beam is also equipped with a time of flight (TOF) device which is started by secondary electrons released at the re-moderator (detected by an off-axis channel electron multiplier) and ended by the PSD signal. A timing efficiency of approximately 10% has been obtained together with a resolution of ≃6 ns [23]. The PSD signal may be set in coincidence with that from the TOF (centered on the arrival time of the incident beam) to obtain a timed PSD distribution. This method reduces the random background to essentially zero.

Experimental method

The total cross section, σ_{T}, is determined using the Beer–Lambert law:

$$\sigma_{\mathrm{T}} = -\frac{k_{\mathrm{B}}T}{Pl}\ln\left(\frac{I}{I_0}\right), \quad (1)$$

where I_0 and I are the incident and transmitted (unscattered) beam intensities respectively, P and T are the gas pressure and temperature respectively, l is the length of the positron path through the gas and k_{B} the Boltzmann constant.

The pressure in the gas cell was measured with a baratron (MKS 627D capacitance manometer), temperature stabilized to 45 °C. A thermal transpiration correction (≃3%) has been applied using the method described in [43], ambient temperature being on average (17 ± 1) °C. A range of gas pressures (0.1–1 Pa for Kr and 4–10 Pa for He) was used to verify pressure independence of the final cross section values, as expected from equation (1) and as seen in figure 2.

In order to ensure similar positron-scattering probabilities outside the cell (estimated to be <1.5%), the I_0 measurements were conducted under the same vacuum conditions as the I measurements by leaking gas into the system through a bypass gas line. The system pressure was monitored throughout the runs using an ion gauge above the remoderator chamber. Consecutive I and I_0 measurements were made, and the average of I_0 on either side of I (and vice versa) was used

[3] In practice, as discussed later in connection with figure 3, further angular discrimination could be applied by examining the dependence of the cross-section upon the beam radius on the PSD.

Table 1. Comparison of relevant experimental parameters associated with systems employed in total cross-section measurements.

Group	Year	System	Angular acceptance θ', E_+	Energy resolution (eV), method	He correction 10 eV	Kr correction 15 eV	Kr correction 40 eV
Toronto [29]	1973	$\vec{B}$ (2–3 G)			⩽0.4%[30]		
Arlington [31]	1979	$\vec{B}$ (4,12 G)	20°	0.2–0.5, TOF	7%		
UCL [32, 33]	1979	$\vec{B}$	35°–20°, (2–20) eV	0.4, TOF	10%	39%	37%
Detroit [34–37]	1980	$\vec{B}$	20°–15°, (1–20) eV	0.1, RPA	6%	30%	46%
Kyoto [38]	1985	$\vec{B}$(8,13 G)	4°, 10 eV	0.2–0.5, TOF	0.5%		
Trento [39, 40]	2006	$\vec{E}+\vec{B}$ (12 G)	17.5°–5.4°, (1–10) eV	0.25, RPA	1%	5%	4%
ANU [41]	2008	$\vec{B}$ (500 G)	18°–4.9°, (1–12) eV	0.07, RPA	1%	5%	4%
Bath [42]	2009	$\vec{B}$ (50 G)	23°–7°, (1–22) eV	0.5, RPA	<8%	13%	
Tokyo [21]	2011	$\vec{E}$	3.2°	0.25, RPA	0.4%		
Current [23]	2015	$\vec{E}$	$\lesssim$2°	1%, TOF	0.1%	⩽1.1%	2%

The symbols $\vec{B}$ and $\vec{E}$ denote whether the beamline employs magnetic or electrostatic transport. In all the cases, except [21] and the current one, the angular acceptance depends on the beam energy E_+. Ensuing systematic errors, $(1/\sigma_T)\int_0^{2\pi}\int_0^{\theta'}(\mathrm{d}\sigma_{el}/\mathrm{d}\Omega)\sin\theta\mathrm{d}\theta\mathrm{d}\phi$ due to the finite angular acceptance θ' have been computed using theoretical predictions as follows: for He using the differential elastic scattering cross sections $(\mathrm{d}\sigma_{el}/\mathrm{d}\Omega)$ of [26, 27], while for Kr the theoretical values in [28] have been used.

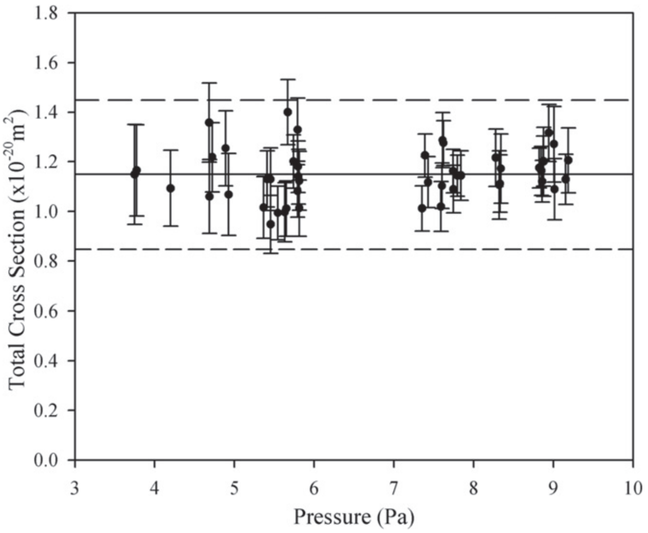

Figure 2. The total cross sections at 100 eV measured for He plotted against gas cell pressure. The lines indicate the mean and three standard deviations.

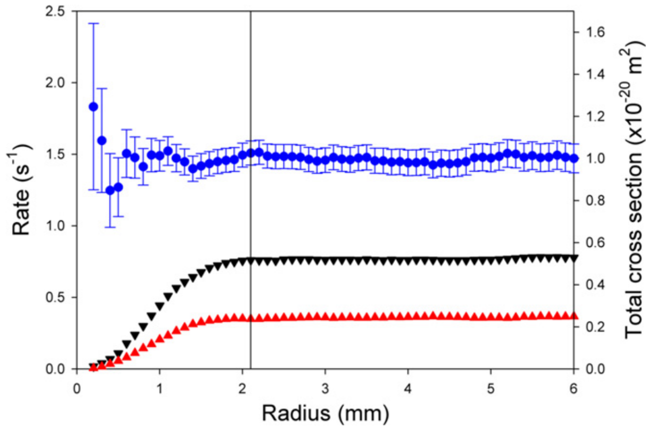

Figure 3. An example of the cumulative radial profiles for I (▲), I_0(▼) and total cross section determinations (●) for a given run at 100 eV for helium. The vertical line shows the selected radius (R_c). The count rate error bars are within the size of the symbols.

to calculate the total cross-section. Measurements of the background were frequently repeated throughout the runs by biasing off the beam with the repelling grid in front of the detector. To minimize possible contaminants introduced into the cell with the gases under investigation (nominal purity: 99.9995% for He and 99.9999% for Kr), the gas lines were periodically baked at temperature of ≃60 °C and repeatedly flushed. A quadrupole mass spectrometer was used to monitor the effective gas purity in the system which was found to be >99.8% throughout the measurements.

Data analysis

In order to discriminate against the possible detection of FSP, the variation of the computed σ_T was examined versus the radius (r) of the beam spot on the PSD. The beam center was determined in two ways: the weighted center of the intensity distribution on the PSD and the center of the timed PSD distribution. Calculation of the total cross section using each center gave results in agreement to within 1% in all cases except at 15 eV in Kr where 5% applies.

The cut-off radius (R_c) of the beam intensity distribution has been investigated using the cumulative radial profiles for I and I_0 after background subtraction (the 'cumulative' profiles are obtained by considering concentric circular regions and summing up the count rates as the radius of the region is increased). An example for a specific run is shown in figure 3, including the variation of the cross section with r. At low radii, large fluctuations in the total cross section can be seen which decrease with increasing r, as this approaches the beam edge. The origin of the fluctuations is partly statistical and partly systematic, the latter related to possible errors in the determination of the centers in each I and I_0 measurement. In this work, the cross section value with the smallest statistical error was chosen, the corresponding (R_c) value agreeing with that of the measured I_0 profile, as illustrated in figure 3.

Using the theoretical differential elastic cross sections of [26, 27] for He and [28] for Kr, it is possible to estimate the

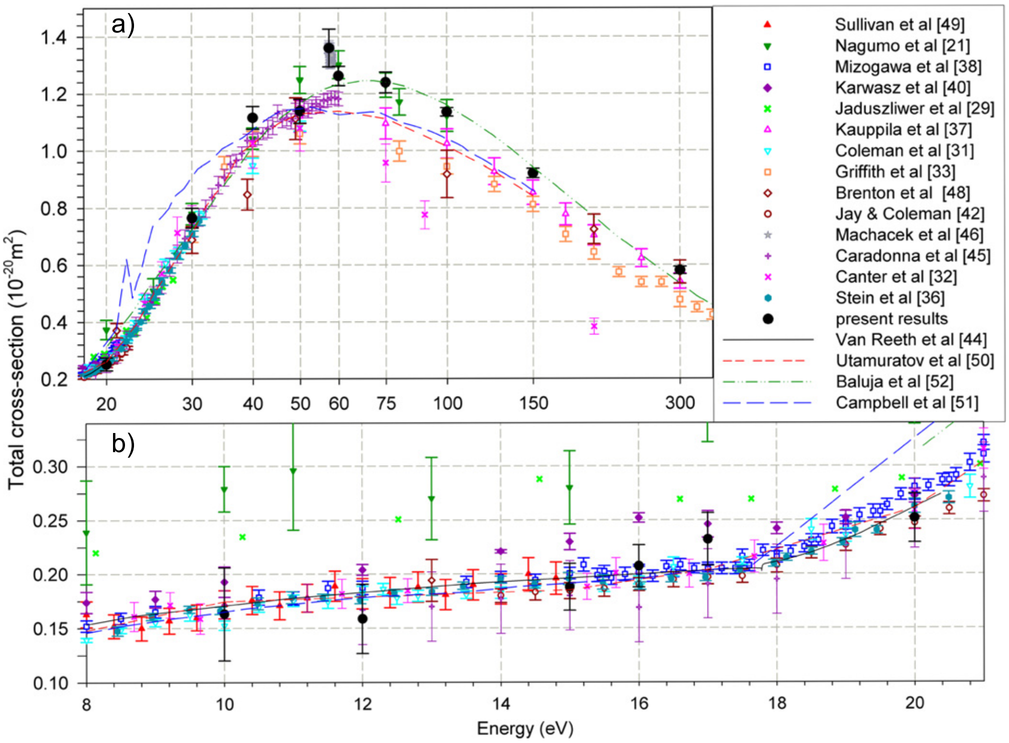

Figure 4. Total cross section for helium: • present work compared with other experimental and theoretical data, as in the legend.

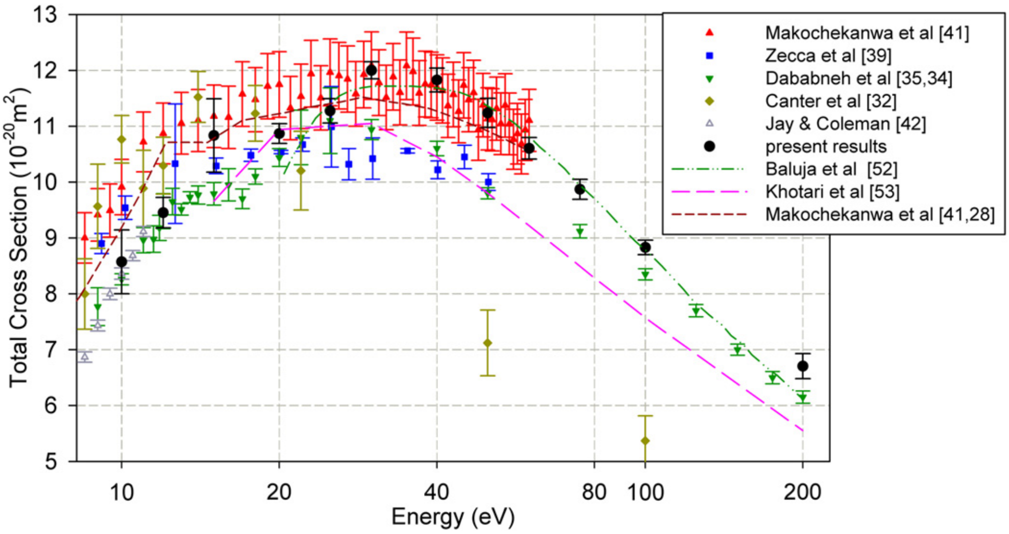

Figure 5. Total cross section for krypton: • present work compared with other experimental and theoretical data, as in the legend.

potential systematic errors due to elastic FSP on the total cross section measurements, theoretical predictions for He being in very good agreement with each other [26, 28, 44]. Table 1 shows a comparison among various experiments. Only the ANU group [41] has explicitly applied this type of correction to their measurements.

Results and discussion

The positron total cross section results for helium and krypton in the energy range (10–300) eV are shown, respectively, in figures 4 and 5 where they are compared with other available experiments and theories.

For He, at 30 eV and above, the present results are systematically larger than those of Griffith *et al* [33], Canter *et al* [32] and Kauppila *et al* [37]; they agree within errors with those of Nagumo *et al* [21] and Caradonna *et al* [45] except in the region 57–60 eV, where they are higher and in better accord with the measurements of Machacek *et al* [46] who searched for—but could not confirm—the resonances predicted to arise from the binding of a positron to doubly excited He [47].

In the range 10–20 eV, the present data disagree with those of Nagumo *et al* [21] and of Jaduszliwer *et al* [29] also performed with a high angular discrimination and, to a smaller extent, of Karwasz *et al* [40]. They are in accord with those of the other experiments shown [31, 36, 38, 42, 48, 49], despite the associated angular discrimination being lower in most cases. This finding supports the theoretical predictions [26, 44, 50] of a small contribution from elastically FSP in this energy range.

Included in figure 4 are the results of various theoretical calculations [44, 50–52]. Below the Ps formation threshold (17.79 eV), a good agreement is found between the current results and those of the close coupling calculation (CC) [51], the convergent close coupling calculation (CCC) [50] and Kohn variational method [44], the same level of agreement extending over the whole range investigated theoretically by the latter [44] and up to 50 eV for CCC [50]. At the highest energies, a systematic deviation (∼10%) is observed from both CCC [50] and CC [51], the latter also being higher than experiments between (20–40) eV. The complex optical potential (COP) calculation of Baluja and Jain [52] is close to the present measurements both in shape and magnitude, except at its lowest (20 eV) and highest (300 eV) energy investigated.

For Kr above 30 eV, the present results are in good agreement with those of Makochekanwa *et al* [41], while they are systematically higher than those of Canter *et al* [32], Dababneh *et al* [34, 35] and Zecca *et al* [39]. Below 15 eV, the data of Canter *et al* [32], Zecca *et al* [39] and Makochekanwa *et al* [41] are generally higher than the present results[4] while a good agreement is found with the results of Dababneh *et al* [34] and Jay and Coleman [42]; given their poorer angular discrimination, this might imply that the predicted corrections in table 1 are too large.

Theoretical calculations for Kr are also shown in figure 5. As in the case of He, a good agreement is found between the present results and the predictions of the COP approach of Baluja and Jain [52]. The accord with the CCC calculation [28, 41] and with the complex scattering potential-ionization theory [53] is weaker.

Conclusion and outlook

We have presented new data for the total cross section of positrons scattering from helium and krypton in the range (10–300) eV obtained with a high (energy-independent) angular discrimination. For both targets, the present results do not show a systematic deviation from previous determinations obtained using magnetic transport and often poorer angular discrimination. We must thus conclude that residual discrepancies among experiments are probably due to other sources of systematic errors. Additionally, in the case of helium, in view of the significant increase in the total cross section between 50 and 57 eV (close to the energies where resonances are predicted to arise due to positron complexes [47]), further investigations may be worthwhile.

Finally, we hope to use the high angular resolution of the present system to investigate polar molecules such as water for which forward elastic scattering currently introduces severe experimental uncertainties [54] and, following a planned upgrade of the positron source, extend measurements to lower energies and to differential cross sections.

The data supporting this publication are available at UCL Discovery (doi: 10.14324/000.ds.1476208).

[4] Makochekanwa *et al* [41] corrected their measurements for the FSP contribution using the theory of [28].

Acknowledgments

We would like to thank Igor Bray and Peter Van Reeth for providing tables of their data and useful discussions, Rafid Jawad and John Dumper for excellent technical assistance, and EPRSC for financial support (EP/E053521/1) and for providing studentships to SEF. AK thanks to the kind hospitality in UCL during his stay and the support of the Hungarian Scientific Research Foundation (OTKA Grant No K104409).

References

[1] Charlton M and Humberston J W 2001 *Positron Physics* (Cambridge: Cambridge University Press)
[2] Surko C M, Gribakin G F and Buckman S J 2005 Low energy positrons interactions with atoms and molecules *J. Phys. B: At. Mol. Opt. Phys.* **38** R57–126
[3] Laricchia G, Armitage S, Kover A and Murtagh D J 2008 Ionizing collisions by positrons and positronium impact on the inert atoms *Adv. At. Mol. Opt. Phys.* **56** 1–47
[4] Laricchia G, Cooke D and Brawley S J 2012 *Radiation Damage in Biomolecular Systems* (Berlin: Springer) ch 8 (doi:10.1007/978-94-007-2564-5)
[5] Laricchia G and Walters H R J 2012 Positronium collision physics *Riv. Nuovo Cimento* **35** 305–51
[6] Walters H R J 1984 Perturbative methods in electron–atom and positron–atom scattering *Phys. Rep. Rev. Sect. Phys. Lett.* **116** 1–02
[7] Humberston J W 1994 Positron and positronium scattering at low energies *Adv. At. Mol. Opt. Phys.* **32** 205–22
[8] Ishida A, Namba T, Asai S, Kobayashi T, Saito H, Yoshida M, Tanaka K and Yamamoto A 2014 New precision measurement of hyperfine splitting of positronium *Phys. Lett.* B **734** 338–334
[9] Vallery R S, Zitzewitz P W and Gidley D W 2003 Resolution of the orthopositronium-lifetime puzzle *Phys. Rev. Lett.* **90** 203402
[10] Jinnouchi O, Asai S and Kobayashi T 2003 Precision measurement of orthopositronium decay rate using SiO_2 powder *Phys. Lett.* B **572** 117
[11] Guessoum N, Jean P and Gillard W 2005 The lives and deaths of positrons in the interstellar medium *Astron. Astrophys.* **436** 171–85
[12] Kohn C and Ebert U 2015 Calculation of beams of positrons, neutrons, and protons associated with terrestrial gamma ray flashes *J. Geophy. Res., Atmos.* **120** 1620–35
[13] Champion C and Le Loirec C 2007 Positron follow-up in liquid water: II. Spatial and energetic study for the most important radioisotopes used in pet *Phys. Med. Biol.* **52** 6605–25
[14] Garcia G and Fuss M C (ed) 2012 *Radiation Damage in Biomolecular Systems* (Berlin: Springer)

[15] Kauppila W E and Stein T S 1990 *Advances in Atomic, Molecular and Optical Physics* vol 26 (San Diego: Academic)

[16] Van Reeth P, Laricchia G and Humberston J W 2005 *Phys. Scr.* **71** C9

[17] Danielson J R, Jones A C L, Natisin M R and Surko C M 2013 Modeling enhancement and suppression of vibrational feshbach resonances in positron annihilation on molecules *Phys. Rev* A **88** 062702

[18] Murtagh D J, Cooke D A and Laricchia G 2009 Excited-state positronium formation from helium, argon, and xenon *Phys. Rev. Lett.* **102** 133202

[19] Cooke D A, Murtagh D J and Laricchia G 2010 Simultaneous ionization and excitation of molecules by positron impact *Phys. Rev. Lett.* **104** 073201

[20] Paludan K *et al* 1997 Ionization of rare gases by particle–antiparticle impact *J. Phys. B: At. Mol. Opt. Phys.* **30** L581–7

[21] Nagumo K, Nitta Y, Hoshino M, Tanaka H and Nagashima Y 2011 Measure of total cross section for positron scattering from He under magnetic-field-free conditions using an electrostatic high-brightness slow positron beam system *J. Phys. Soc. Japan* **80** 064301

[22] Nagumo K, Nitta Y, Hoshino M, Tanaka H and Nagashima Y 2012 Magnetic-field-free measurements of the total cross sections for positron scattering from neon *Eur. Phys. J.* D **66** 81

[23] Kövér Á, Williams A I, Murtagh D J, Fayer S E and Laricchia G 2014 An electrostatic brightness-enhanced timed positron beam for atomic collision experiments *Meas. Sci. Technol.* **25** 075013

[24] Williams A I, Murtagh D J, Fayer S E, Andersen S L, Chevallier J, Kövér Á, Van Reeth P, Humberston J W and Laricchia G 2015 Moderation and diffusion of positrons in tungsten meshes and foils *J. Appl. Phys.* **118** 105302

[25] Mathur B P *et al* 1975 Calculations of effusive-flow patterns: iii. Scattering chambers with thin circular apertures *Phys. Rev.* A **11** 830–3

[26] Van Reeth P 2015 private communication

[27] Fursa D V and Bray I 1995 Calculation of electron–helium scattering *Phys. Rev.* A **52** 1279

[28] Fursa D and Bray I 2012 Convergent close-coupling method for positron scattering from noble gases *New J. Phys.* **14** 035002

[29] Jaduszliwer B and Paul D A L 1973 Positron–helium scattering cross-sections and phase-shifts below 19 eV *Can. J. Phys.* **51** 1565–72

[30] Charlton M 1985 Experimental studies of positrons scattering in gases *Rep. Prog. Phys.* **48** 737–94

[31] Coleman P G, McNutt J D, Diana L M and Burciaga J R 1979 Scattering of low-energy positrons by helium and neon atoms *Phys. Rev.* A **20** 145–53

[32] Canter K F, Coleman P G, Griffith T C and Heyland G R 1973 The measurement of total cross sections for positrons of energies 2–400 eV in He, Ne, Ar, and Kr *J. Phys. B: At. Mol. Phys.* **6** L201

[33] Griffith T C, Heyland G R, Lines K S and Twomey T R 1979 Total cross-sections for the scattering of positrons by helium, neon, and argon at intermediate energies *Appl. Phys* **19** 431–7

[34] Dababneh M S, Kauppila W E, Downing J P, Laperriere F, Pol V, Smart J H and Stein T S 1980 Measurements of total scattering cross sections for low-energy positrons and electrons colliding with krypton and xenon *Phys. Rev.* A **22** 1872–7

[35] Dababneh M S, Hsieh Y F, Kauppila W E, Pol V and Stein T S 1982 Total-scattering cross-section measurements for intermediate-energy positrons and electrons colliding with Kr and Xe *Phys. Rev.* A **26** 1252–9

[36] Stein T S, Kauppila W E, Pol V, Smart J H and Jesion G 1987 Measurements of total scattering cross sections for low-energy positrons and electrons colliding with helium and neon atoms *Phys. Rev.* A **17** 1600–8

[37] Kauppila W E, Stein T S, Smart J H, Dababneh M S, Ho Y K, Downing J P and Pol V 1981 Measurements of total scattering cross sections for intermediate-energy positrons and electrons colliding with helium, neon, and argon *Phys. Rev.* A **24** 725–42

[38] Mizogawa T, Nakayama Y, Kawaratani T and Tosaki M 1985 Precise measurements of positron–helium total cross sections from 0.6 to 22 eV *Phys. Rev.* A **31** 2171–9

[39] Zecca A, Chiari L, Trainotti E, Fursa D V, Bray I and Brunger M J 2011 Experimental determination of the scattering length for positron scattering from krypton *Eur. Phys. J.* D **64** 317–21

[40] Karwasz G P 2005 Positrons—an alternative probe to electron scattering *Eur. Phys. J.* D **35** 267–78

[41] Makochekanwa C *et al* 2011 Low-energy positron interactions with krypton *Phys. Rev.* A **83** 032721

[42] Jay P M and Coleman P G 2010 Coupling between positronium formation and elastic positron-scattering channels in the rare gases *Phys. Rev.* A **82** 012701

[43] Takaishi T and Sensui Y 1963 Thermal transpiration effect of hydrogen, rare gases and methane *Trans. Faraday Soc.* **59** 2503–14

[44] Van Reeth P and Humberston J W 1999 Elastic scattering and positronium formation in low-energy positron–helium collisions *J. Phys. B: At. Mol. Opt. Phys.* **32** 3651–67

[45] Caradonna P, Jones A, Makochekanwa C, Slaughter D S, Sullivan J P, Buckman S J, Bray I and Fursa D V 2009 High-resolution positron scattering from helium: grand total and positronium-formation cross sections *Phys. Rev.* A **80** 032710

[46] Machacek J R, Boadle R, Buckman S J and Sullivan J P 2012 Search for positron quasibound states in the doubly excited region of the helium atom *Phys. Rev.* A **86** 064702

[47] Bromley M W J, Mitroy J and Varga K 2014 Positron attachment to the he doubly excited states *Phys. Rev. Lett.* **109** 063201

[48] Brenton A G, Dutton J, Harris F M, Jones R A and Lewis D M 1977 Experimental determination of total scattering cross sections for positron–helium collisions *J. Phys. B: At. Mol. Phys.* **10** 2699–710

[49] Sullivan J P, Makochekanwa C, Jones A, Caradonna P and Buckman S J 2008 High-resolution, low-energy positron scattering from helium: measurements of the total scattering cross section *J. Phys. B: At. Mol. Opt. Phys.* **41** 081001

[50] Utamuratov R, Kadyrov A S, Fursa D V, Bray I and Stelbovics A T 2010 Multiconfigurational two-centre convergent close-coupling approach to positron scattering on helium *J. Phys. B: At. Mol. Opt. Phys.* **43** 125203

[51] Campbell C P, McAlinden M T, Kernoghan A A and Walters H R J 1998 Positron collisions with one- and two-electron atoms *Nucl. Instrum. Methods Phys. Res.* B **143** 41–56

[52] Baluja K L and Jain A 1992 Positron scattering from rare gases (He, Ne, Ar, Kr, Xe, and Rn): total cross sections at intermediate and high energies *Phys. Rev.* A **46** 1279–90

[53] Kothari H N and Joshipura K N 2012 Total (complete) and ionization cross-sections of argon and krypton by positron impact from 15 to 2000 eV—theoretical investigations *Pramana J. Phys.* **79** 445–442

[54] Tattersall W, Chiari L, Machacek J R, Anderson E, White R D, Brunger M J, Buckman S J, Garcia G, Blanco F and Sullivan J P 2014 Positron interactions with water-total elastic, total inelastic, and elastic differential cross section measurements *J. Chem. Phys.* **140** 044320